JCTC Journal of Chemical Theory and Computation

Conjugated Molecules Described by a One-Dimensional Dirac Equation

Matthias Ernzerhof* and Francois Goyer

Département de Chimie, Université de Montréal, C. P. 6128 Succursale A, Montréal, Québec H3C 3J7, Canada

Received January 3, 2010

Abstract: Starting from the Hückel Hamiltonian of conjugated hydrocarbon chains (ethylene, allyl radical, butadiene, pentadienyl radical, hexatriene, etc.), we perform a simple unitary transformation and obtain a Dirac matrix Hamiltonian. Thus already small molecules are described exactly in terms of a discrete Dirac equation, the continuum limit of which yields a one-dimensional Dirac Hamiltonian. Augmenting this Hamiltonian with specially adapted boundary conditions, we find that all the orbitals of the unsaturated hydrocarbon chains are reproduced by the continuous Dirac equation. However, only orbital energies close to the highest occupied molecular orbital/lowest unoccupied molecular orbital energy are accurately predicted by the Dirac equation. Since it is known that a continuous Dirac equation describes the electronic structure of graphene around the Fermi energy, our findings answer the question to what extent this peculiar electronic structure is already developed in small molecules containing a delocalized π-electron system. We illustrate how the electronic structure of small polyenes carries over to a certain class of rectangular graphene sheets and eventually to graphene itself. Thus the peculiar electronic structure of graphene extends to a large degree to the smallest unsaturated molecule (ethylene).

Introduction

Presently, graphene is at the center of numerous investigations (for recent reviews see, e.g., refs 1–5). The remarkable features of graphene, such as its conductance properties,[3] can be attributed to its peculiar electronic structure. In the simplest Hückel description,[6] accounting for nearest-neighbor coupling, the dispersion relation close to the Fermi energy is linear, and this energy region can be described[7,8] by a two-dimensional (2D) Dirac equation of massless fermions. Recently, one-dimensional (1D) graphene-based systems have become accessible to experiments[2,9] as well as zero-dimensional ("molecular") ones.[2,10,11]

The question that we strive to answer in the present work is whether the electronic structure of graphene has precursors in the molecular domain. Here we refer to the unsaturated hydrocarbon chains defined in Figure 1 as polyenes. Within the Hückel model (nearest-neighbor coupling), we show that these polyenes are described by a 1D, discrete Dirac equation

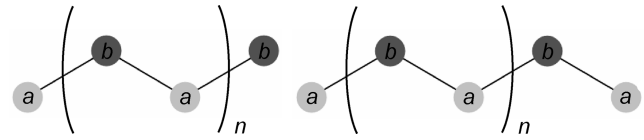

Figure 1. Schematic representation of the unsaturated hydrocarbons investigated. Even- (left) as well as odd-numbered chains are considered. The artificial subdivision into sublattices of *a*- and *b*-type carbon atoms is indicated as well.

of massless ($m = 0$) particles. The continuum limit of this discrete equation yields a 1D Dirac equation that reproduces the Hückel orbitals exactly (up to a gauge transformation and a normalization factor). The orbital energies of orbitals close to the highest occupied molecular orbital (HOMO) and lowest unoccupied molecular orbital (LUMO) are well represented as well by the continuous equation. The continuous, 1D Dirac equation ($m = 0$) contains a Pauli spin matrix:

$$\sigma = \begin{pmatrix} 0 & -i \\ i & 0 \end{pmatrix} \tag{1}$$

which multiplies the derivative operator $d = d/dx$, i.e.:

* Corresponding author. E-mail: Matthias.Ernzerhof@UMontreal.ca.

10.1021/ct1000044
Published on Web 05/12/2010

$$-iv_F\sigma d\phi = \varepsilon\phi \tag{2}$$

ϕ is a two-component pseudospinor:

$$\phi = \begin{pmatrix}\phi_u\\ \phi_d\end{pmatrix} \tag{3}$$

and v_F the Fermi velocity. As we will show below, this equation, which is often referred to as Weyl equation,[12] is the continuous limit of the transformed Hückel Hamiltonian of linear polyenes. The fact that these molecules are described by a Dirac equation offers a new perspective for their electronic structure. A recent article[13] dealing with infinite, linear carbon chains arrives at an equivalent Dirac equation for the description of the system close to the Fermi energy.

A question that arises in this context is whether the electronic structure of the polyenes can be somehow related to the electronic structure of graphene or finite parts thereof. We provide a positive answer to this question by examining rectangular pieces of graphene. For a particular class of graphene rectangles, the electronic structure near the Fermi energy is essentially 1D and identical to the electronic structure of polyenes.

Polyene Described in Terms of a 1D Dirac Equation. Now we show how the Dirac equation, described in the introduction, emerges as the continuum limit of the Hückel matrix for polyene. To this end, we start from a matrix of unspecified dimension. We regroup the atoms into two bipartite sublattices (cf. Figure 1) such that every other atom belongs to the sublattice of *a* atoms, and the remaining ones form the *b* sublattice. To emphasize this division, we use the variable *a* for the diagonal matrix element of the atoms belonging to the *a* sublattice. Similarly, *b* denotes the diagonal element of the atom in the *b* sublattice, even though the numerical value of both these parameters is zero:

$$\mathbf{H} = \begin{pmatrix}
\ddots & & & & & & & & \\
 & a & t & & & & & & \\
 & t & b & t & & & & & \\
 & & t & a & t & & & & \\
 & & & t & b & t & & & \\
 & & & & t & a & t & & \\
 & & & & & t & b & & \\
 & & & & & & & \ddots &
\end{pmatrix} \tag{4}$$

where *t* is the hopping parameter. An appropriate permutation of the basis functions separates the atoms of the *a* and *b* lattice. The resulting $\tilde{\mathbf{H}}$ reads

$$\tilde{\mathbf{H}} = \begin{pmatrix}
\ddots & & & & & & & & \\
 & a & & & t & t & & & \\
 & & a & & & t & t & & \\
 & & & a & & & t & \ddots & \\
 & & & & \ddots & & & & \\
\ddots & t & & & b & & & & \\
 & t & t & & & b & & & \\
 & & t & t & & & b & & \\
 & & & \ddots & & & & \ddots &
\end{pmatrix} \tag{5}$$

$\tilde{\mathbf{H}}$ can be converted into the discrete version of the Dirac Hamiltonian in eq 2 through application of a gauge transformation **G**. This transformation consists of multiplying the coefficient of every second atom of the *a* lattice as well as *b* lattice with −1. If we denote the initial coefficient vector by **C**, then the new, transformed coefficient vector will be given by

$$\mathbf{Q} = \mathbf{GC} \tag{6}$$

Q represents the envelope function of **C**. For orbitals with energies close to the HOMO and LUMO, the short-range variations in **C** are eliminated by **G**, and only the long-range variations are retained in **Q**. This point is illustrated in the orbital plots provided below. A corresponding modification of the Hamiltonian matrix, compensating for the transformation of the wave function, yields the matrix operator **D**:

$$\mathbf{D} = \mathbf{GHG}^{-1} = \begin{pmatrix}
\ddots & & & & & & & & \\
 & a & & & -t & t & & & \\
 & & a & & & -t & t & & \\
 & & & a & & & -t & \ddots & \\
 & & & & \ddots & & & & \\
\ddots & -t & & & b & & & & \\
 & t & -t & & & b & & & \\
 & & t & -t & & & b & & \\
 & & & \ddots & & & & \ddots &
\end{pmatrix} \tag{7}$$

Keeping in mind that $v_F = -2t$, **D** can be identified as the discretized version of $-iv_F\sigma d/dx$ appearing in eq 2. The solutions of the continuous Dirac equation (eq 2) are now discussed in some detail and compared to the eigenfunctions obtained with the Hückel approach, or equivalently, to the eigenfunctions of **D**.

Solutions for Particular Systems: Introducing Boundary Conditions. The eigenfunctions of the continuous Dirac equation (eq 2) and their respective eigenvalues are of the form:

$$\phi^{\pm} = \frac{1}{\sqrt{2}}e^{ikx}\begin{pmatrix}1\\ \pm i\end{pmatrix}, \qquad \varepsilon = \pm v_F k \tag{8}$$

The wave vector *k* in this equation is a real variable. Similar to the 2D case, the eigenfunctions exhibit helicity.[4] This means that solutions describing forward-moving particles have a defined pseudospin orientation $s^+ = (\frac{1}{+i})$, whereas backward-traveling particles have the opposite pseudo spin $s^- = (\frac{1}{-i})$. To arrive at this result, one can calculate the probability current density *j* to obtain, $j = v_F(\phi^*\sigma\phi - \phi\sigma\phi^*)$, and note that $\sigma s^+ = s^+$ and $\sigma s^- = -s^-$. The equation for *j* also shows that even if the wave vector in eq 8 is proportional to the energy, the particle velocity is constant and equal to v_F. In relativistic quantum mechanics this behavior corresponds to massless particles that move with the speed of light. Here we are particularly interested in finding the wave functions of finite systems, and the periodic solutions of eq 2 are not a suitable starting point. Real solutions ϕ^s and ϕ^c that are linear combinations of the complex ones (ϕ^+ and ϕ^-) are appropriate

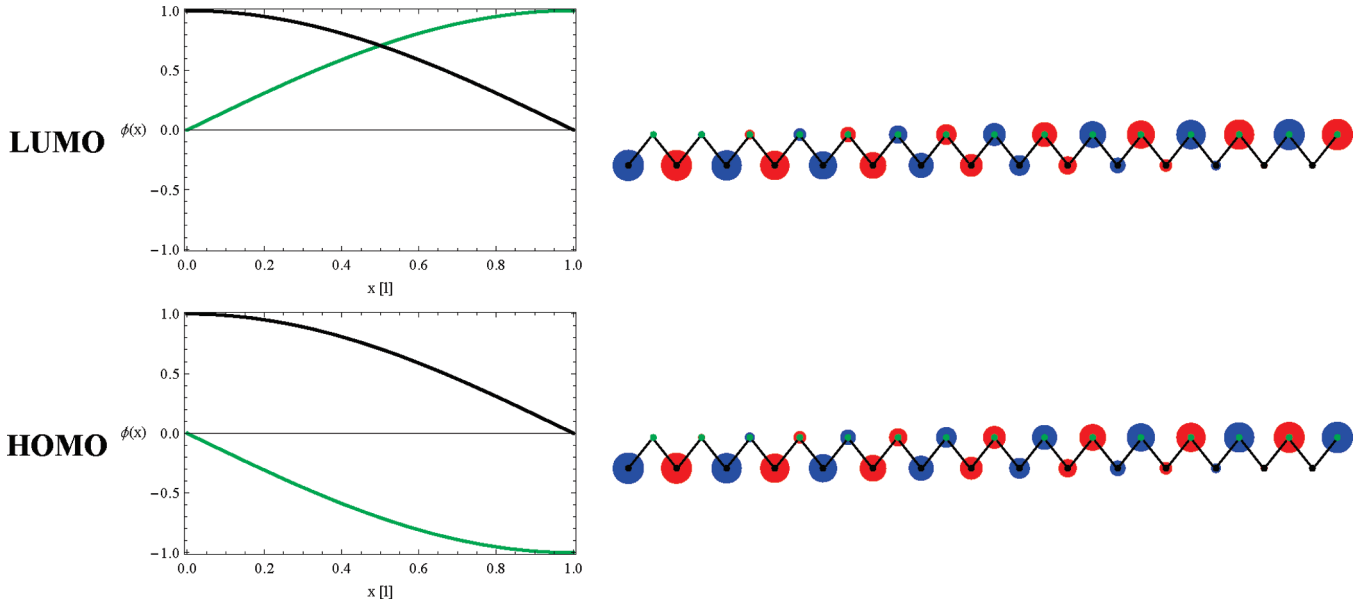

Figure 2. Massless Dirac particle in a box. The $k = -((\pi/2)/l)$, (where $n = -1$) and $k = ((\pi/2)/l)$ (with $n = 0$) wave functions are displayed on the left (ϕ_u is represented by the green and ϕ_d by the black curve) and compared to the HOMO (lower orbital) and LUMO (upper orbital) of a polyene chain with 30 atoms (i.e., $N = even$). The continuous solutions are accurate representations of the orbital envelope functions.

$$\phi^s = \begin{pmatrix} \sin(kx) \\ \cos(kx) \end{pmatrix} \tag{9}$$

$$\phi^c = \begin{pmatrix} \cos(kx) \\ -\sin(kx) \end{pmatrix} \tag{10}$$

These states are not pure pseudospin states anymore. In the continuum limit, the equivalent of a polyene would be a finite box terminated to the right and left by infinite potential barriers. Apparently, the appropriate boundary conditions are that the wave function vanishes at the borders (at $x = 0$ and $x = l$) of the box, i.e., $\phi(x = 0) = \phi(x = l) = 0$. Naively, one would apply this condition to the two components of the pseudospinor. Here, however, we arrive at the continuous model as a limit of discrete systems, and the boundary conditions are also defined through a limiting procedure. Thus, each of the two components represents the wave function on a set of points the two of which are complementary. Therefore, we have to distinguish between two cases: (i) the one where each of the sets contains one end point, implying that the number of atoms (N) in the chain is even, and (ii) the case where one set includes both points 0 and l, which would correspond to an odd number of atoms in the chain. Starting with (i), we suppose that the domain of the up component ϕ_u in the wave function $\phi = (\phi_u,\phi_d)$ starts at the left boundary of the box and terminates before the right boundary is reached. Similarly, the domain of points for the down component (ϕ_d) does not contain the boundary point on the left but the one on the right. This choice excludes eq 10, and only eq 9 yields solutions that vanish at the boundary if

$$k = \frac{(n + (1/2))\pi}{l}, \qquad n = ..., -2, -1, 0, 1, 2, ... \tag{11}$$

To illustrate these solutions, we choose $n = -1$ and 0 and plot the two components of the wave function (Figure 2). For comparison, we also plot the HOMO and LUMO of a $N = 30$ polyene chain. Clearly, the solutions of the continuous Dirac equation yield an accurate model for the envelope function of the HOMO (corresponding to $n = -1$) and the LUMO orbital (corresponding to $n = 0$). To better establish the connection between the solutions of the discrete equation and the ones of the continuous equation, we note that an N-atom chain represents a box that has been discretized with $N + 2$ points. Two of these points, one on both the left- and the right-hand side, lie on the boundary of the box where the wave function vanishes. Correspondingly, the N remaining points (associated with the N atoms) are all inside of the box and have nonvanishing coefficients in general.

Next we consider the case (ii) where the domain of ϕ_u contains both end points. This would correspond to a carbon chain with an odd number of atoms. Since the boundary condition is only relevant for one of the two discrete sets of points, i.e., the one ϕ_u is defined on, only this component has to satisfy the boundary conditions and thus defines the admissible values of k:

$$k = \frac{n\pi}{l}, \qquad n = ..., -2, -1, 0, 1, 2, ... \tag{12}$$

In this case (see Figure 3), the continuous model also reproduces the envelope of the displayed Hückel orbitals.

Another 1D system of interest is a ring where the wave function satisfies periodic boundary conditions. The solutions of the continuous Dirac equation can only be compared to the orbitals of a circular molecule, whose number of atoms is a multiple of 4. This condition arises because the transformation $\mathbf{G}$ (eq 6) imposes that, on each sublattice, every second coefficient is multiplied by -1. For this transformation to be unique on a ring, it has to contain a number of atoms that is a multiple of 4. Both solutions of

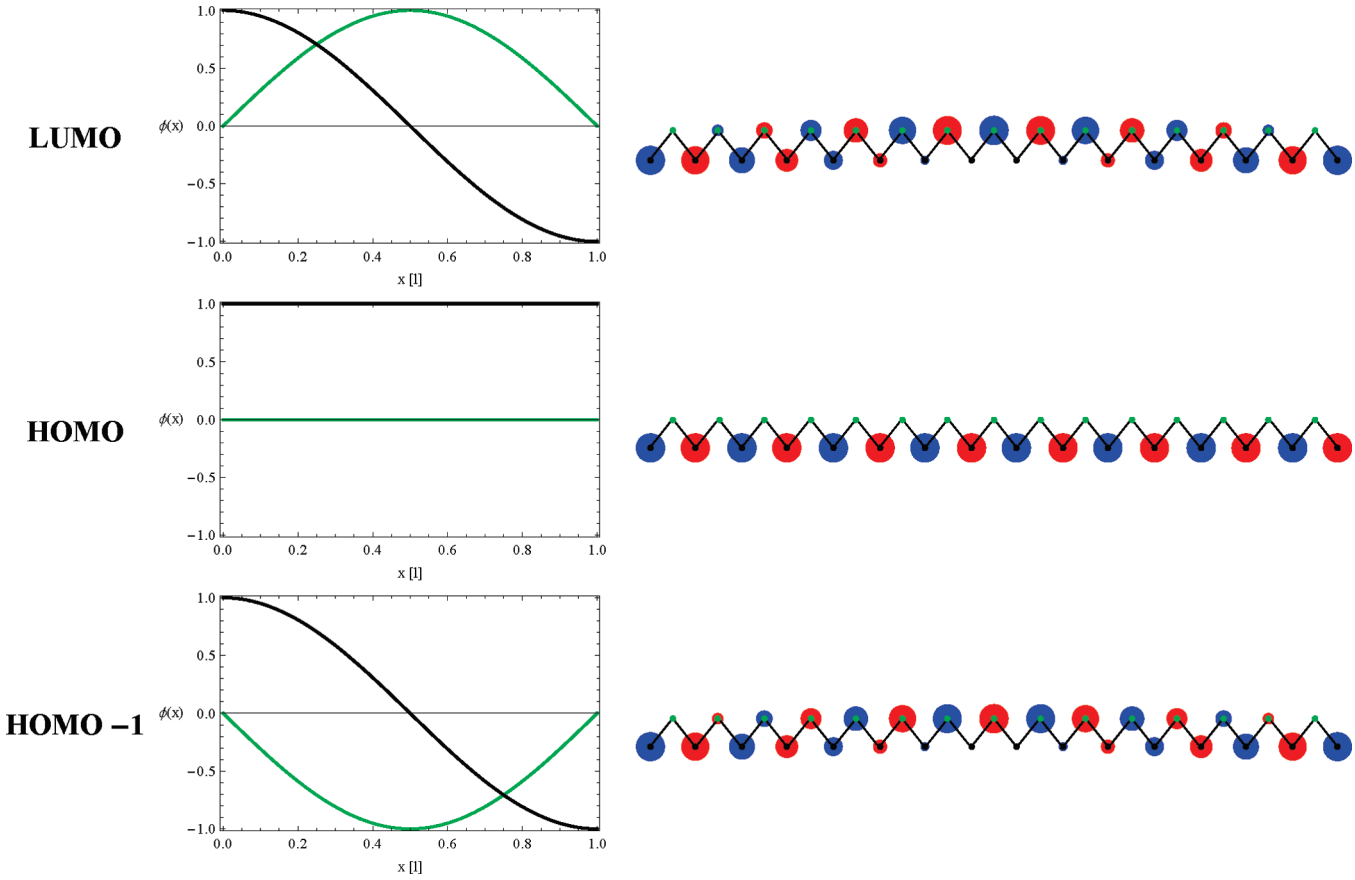

Figure 3. Massless Dirac particle in a box. The left part illustrates the solutions of the continuous Dirac equation with $k = -\pi/l$, 0, and π/l (corresponding to $n = -1,\ 0,\ 1$), from the bottom up, respectively; ϕ_u is represented by the green and ϕ_d by the black curve. For comparison, the corresponding orbitals of polyene with 31 atoms are also shown. The singly occupied orbital is in the middle, while its energetic neighbors are shown below and above. Again, the envelope function of the orbitals is reproduced by the continuous solutions.

the continuous Dirac equation, ϕ^s and ϕ^c, satisfy the periodic boundary conditions if

$$k = n\frac{2\pi}{l}, \qquad n = ..., -2, -1, 0, 1, 2, ... \qquad (13)$$

As in the nonperiodic case, the solutions of the Dirac equation correspond to the envelope functions of the Hückel orbitals. Alternatively, the complex solutions ϕ^- and ϕ^+ can also be employed together with eq 13 to describe the system. In this case the solutions are helical, a property shared with the massless fermions found in infinite graphene. Cyclic molecules with $4n$ electrons are anti-aromatic, thus for finite systems, helicity and anti-aromaticity appear to coincide.

Small Polyenes. Now we turn to the question of how long a polyene has to be to be well represented by the continuum model. To address this issue, we compare the dispersion relation of the continuous Dirac equation to the Hückel energy distribution of polyenes. The latter distribution is known analytically:

$$E_n = 2t\cos\left(\frac{\pi n}{N+1}\right), \qquad n = 1, 2, ..., N \qquad (14)$$

We introduce a wave vector k in eq 14 in the canonical way. Changes in the wave vector are $(\pi\Delta n)/(N+1)$, as the index of the states changes by Δn. Furthermore, the origin of the wave vector is shifted by $-\pi/2$ to account for the gauge transformation. The resulting dispersion relation:

$$E(k) = -2t\sin(k), \qquad k \in \left[-\frac{\pi}{2}, \frac{\pi}{2}\right] \qquad (15)$$

is compared (Figure 4) to the corresponding relation of the continuous Dirac equation. For small values of $|k|$, the

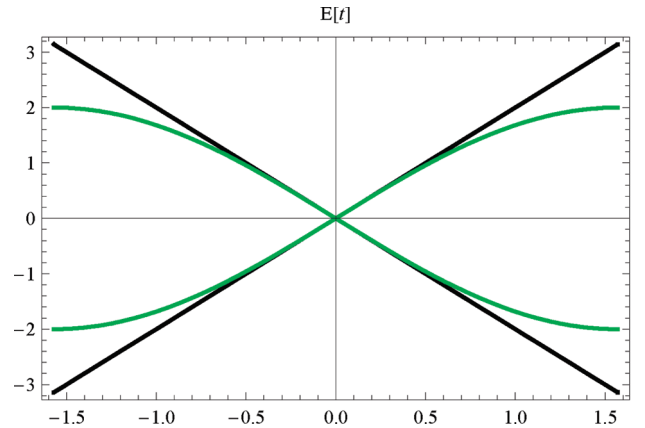

Figure 4. Energy dispersion relation of finite polyenes (green curves) compared to the dispersion relation of the continuous Dirac equation (black lines). Note that the argument k in eq 15 has been replaced by $-k$ to obtain the second green graph. This has been done to mimic the degeneracy that is present in the infinite or periodic system but absent in the nonperiodic, finite one.

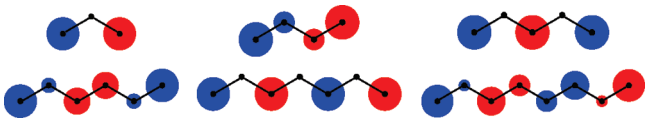

Figure 5. HOMOs of *N*-atom polyenes ($N = 3, ..., 8$). The odd-numbered chains all show identically structured HOMOs having a vanishing contribution on one sublattice. Similarly, the even-numbered chains have HOMOs, whose envelope describes a quarter wave on each of the sublattices.

dispersion relations are almost identical, and they differ in the large-$|k|$ regime, where the Hückel spectrum exhibits the known quadratic behavior.

A related question is how similar the Hückel orbitals are to the solutions of the Dirac equation? This question has a strikingly simple answer. For all values of N they are, up to the gauge transformation $\mathbf{G}$ and a normalization factor, identical. More precisely, if we take a solution of the continuous Dirac equation (subject to the proper boundary conditions) and represent it on an equidistant grid of $N + 2$ points, then the resulting orbital is related to an orbital of a polyene with N atoms by a gauge transformation. This can be readily verified by acting with $\mathbf{D}$ on $\mathbf{Q}$, where $\mathbf{Q}$ is a grid representation of ϕ_s defined in eq 9. Then components, such as $t\sin(k(n+2)) - t\sin(kn)$ and $t\cos(k(n+2)) - t\cos(kn)$, of the resulting vector are examined. By exploiting trigonometric identities, these expressions can be converted to

$$\begin{aligned} t\sin(kn) - t\sin(k(n+2)) &= -2t\cos(k(n+1))\sin(k) \\ &= E(k)\cos(k(n+1)) \end{aligned} \tag{16}$$

and

$$\begin{aligned} t\cos(k(n+2)) - t\cos(kn) &= -2t\sin(k(n+1))\sin(k) \\ &= E(k)\sin(k(n+1)) \end{aligned} \tag{17}$$

showing that the discrete Dirac equation is satisfied. This finding is analogous to the known[14] fact that a discretization of the free-electron model yields the exact Hückel orbitals.

In Figure 5, we provide the Hückel HOMOs of a number of polyenes with $N = 3, ..., 8$. As can be guessed and verified analytically, they are identical to the solutions of the continuous Dirac equation modulo a gauge transformation.

Relation to Finite Graphene Ribbons. The electronic structure of the polyenes discussed above carries over to a surprising degree to finite graphene ribbons[15–17] of a certain width. In detail, we consider a symmetric, rectangular piece of graphene with two armchair edges (along the longitudinal direction) and two zigzag edges. The length of the ribbons is assumed to be large compared to their width. Recently, the edge states that appear in finite graphene ribbons and other finite shapes have been investigated extensively, among these studies are refs 18–27. These edge states are typically found along zigzag borders. Electronic structure calculations taking electron interaction into account show that the edge states can result in spin polarization since they are preferentially occupied with electrons of a particular spin orientation.[18,26] By keeping the width of the ribbon small compared to its length, we reduce the number of edge states and the associated complexity.

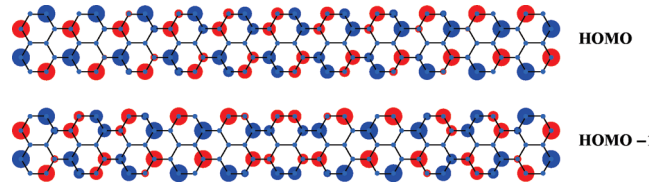

Figure 6. Shown are the HOMO and the HOMO-1 of a graphene rectangle which is two benzene rings wide. Both orbitals exhibit a nodal plane in longitudinal direction which effectively separates the system into two polyene chains. These polyene chains in turn exhibit envelope functions corresponding to solutions of the continuous Dirac equation.

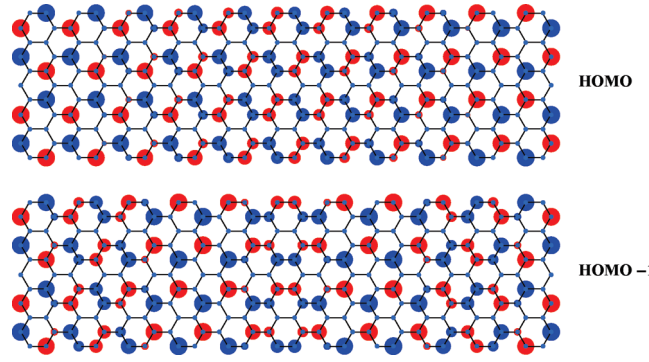

Figure 7. Orbitals of a graphene rectangle which is five benzene rings wide. Omitting states localized at the zigzag boundaries (i.e., edge states discussed in the text), the HOMO and the HOMO-1 are displayed in the figure. Effective polyene chains are clearly visible in both orbitals.

The narrowest ribbon, conforming to the above listed restrictions, is shown in Figure 6. It exhibits no edge states, and we recover the electronic structure already discussed for polyene. In the examples considered, the transverse degree of freedom is effectively frozen since excitations in transverse direction require too much energy. Furthermore, there is no binding or antibinding in the transverse direction since the states of interest have an energy close to 0. As one might suspect, the pattern observed in Figure 6 repeats itself in ribbons, whose width is given by $3n + 2$ benzene rings. An example is shown in Figure 7, where $n = 1$. This ribbon exhibits four edge states with energies at or close to 0. These states are localized at the zigzag edged, and here we neglect their impact on the electronic structure, which is reasonable if the length of the ribbon is small compared to its width. Infinite armchair graphene ribbons with a width of $3n + 2$ benzene rings are known to be metallic in the Hückel model (see, e.g. refs 17, 28–31 and references therein). In view of our discussion this is not surprising since, in the limit of an infinite ribbon length, the 1D Dirac equation, describing the dispersion relation around the Fermi energy, yields a vanishing band gap. It should be mentioned, however, that more sophisticated density functional theory calculations[32,33] yield small band gaps for armchair ribbons.

Armchair ribbons other than the ones discussed here exhibit, in general, a coupling between the longitudinal polyene chains, which results in a band gap even at the

Hückel level. Furthermore, we recall that, except for the narrowest armchair ribbons, edge states play a role and alter the dispersion relation close to the Fermi energy. Increasing the length of the ribbon renders these surface effects less and less important. Detailed computational studies of the transition of the electronic structure from finite ribbons to graphene are provided in refs 18 and 22.

Summary and Conclusion

Maybe the most important result obtained here is that the Hückel Hamiltonian can be rigorously transformed into a discrete Dirac Hamiltonian. Even the continuous limit of the discrete Hamiltonian, yielding the 1D Dirac equation, results in the exact polyene orbitals. The boundary conditions, accompanying the continuous Dirac operator, play a crucial role. They are somewhat involved since they are defined by taking the limit of the conditions applied to discrete systems. Straight forward application of particle-in-a-box boundary conditions does not yield a solution for the Dirac equation of massless particles.

For graphene, the electronic structure close to the Fermi energy is accurately described by the Dirac equation. This result is arrived at (see, e.g., ref 4) by linearizing a wave vector dependent Schrödinger equation that is subjected to periodic boundary conditions. Adding to these findings, here we consider finite polyene chains and show that a surprisingly simple transformation turns the Hückel matrix of a finite polyene into a discrete Dirac Hamiltonian.

Neglecting edge states (see the discussion in the previous section), we find that graphene rectangles that have a width (given in units of benzene rings) of $3n + 2$ exhibit no coupling between longitudinal and transverse degrees of freedom in orbitals with energies close to 0. These systems can be described as effective polyene chains by the 1D Dirac equation. For armchair graphene ribbons of infinite length, it is known that, at the Hückel level, $3n + 2$ ribbons have a vanishing band gap.[17] This appears to be a simple consequence of the structure of the wave function revealed here. Increasing the length and width of the $3n + 2$ ribbon, we eventually arrive at graphene where what we refer to as the longitudinal direction is now one of three equivalent orientations, since graphene has a six-fold rotational symmetry.

Graphene is regarded as a model system[3] for quantum electrodynamics (for an introduction see, e.g., ref 12). Here, we demonstrate that even small molecules can serve to illustrate features of the Dirac equation subject to finite-system boundary conditions. There appears to be a considerable similarity between finite conjugated systems, such as the ones discussed here, and graphene. It is puzzling that involved ideas of quantum electrodynamics can be illustrated in terms of the Hückel model of polyenes. However, we should add that, in finite systems, there are boundary effects, such as edge states, discussed in the previous section, that have no analogue in graphene. Furthermore, graphene is a two-dimensional (2D) system, and therefore, there are topological effects that have no counterpart in one-dimensional (1D) systems. An example is the Berry phase that the wave function of graphene can acquire if the wave vector varies along closed loops.[4]

The free-electron model is often employed to qualitatively explain the behavior of π-electrons in polyene. For example, this model has been used recently[34] to investigate the electron transport properties of conjugated systems. Since the free-electron model is based on a differential equation and not on a matrix equation, its solutions can be obtained analytically. However, its quadratic dispersion relation does not correctly reproduce the energy level spacing of polyenes around the highest occupied molecular orbital/lowest unoccupied molecular orbital (HOMO/LUMO) energies. The discrete Dirac equation presented here results in an alternative continuum model given by the 1D Dirac equation. This equation yields a linear dispersion relation and rectifies a problem of the free-electron model. Furthermore, the Dirac energy spectrum is symmetric with respect to the midpoint between the HOMO and the LUMO. This is a feature of the Hückel spectrum as well that is not reproduced by the conventional free-electron model.

Acknowledgment. We would like to thank P. Rocheleau whose critical reading of the manuscript lead to various improvements. M.E. is indebted to Didier Mayou for inspiring discussions which sparked his interest in graphene. Furthermore, we gratefully acknowledge financial support provided by Natural Sciences and Engineering Research Council (NSERC).

References

(1) Novoselov, K. S.; Geim, A. K.; Morozov, S. V.; Jiang, D.; Zhang, Y.; Dubonos, S. V.; Grigorieva, I. V.; Firsov, A. A. *Science* **2004**, *306*, 666–669.

(2) Geim, A. K.; Novoselov, K. S. *Nat. Mater.* **2007**, *6*, 183–191.

(3) Geim, A. K. *Science* **2009**, *324*, 1530–1534.

(4) Neto, A. H. C.; Guinea, F.; Peres, N. M. R.; Novoselov, K. S.; Geim, A. K. *Rev. Mod. Phys.* **2009**, *81*, 109–162.

(5) Rao, C.; Sood, A.; Subrahmanyam, K.; Govindaraj, A. *Angew. Chem., Int. Ed.* **2009**, *48*, 7752–7777.

(6) Wallace, P. R. *Phys. Rev.* **1947**, *71*, 622–634.

(7) Semenoff, G. W. *Phys. Rev. Lett.* **1984**, *53*, 2449–2452.

(8) DiVincenzo, D. P.; Mele, E. J. *Phys. Rev. B: Condens. Matter Mater. Phys.* **1984**, *29*, 1685–1694.

(9) Novoselov, K. S.; Jiang, Z.; Zhang, Y.; Morozov, S. V.; Stormer, H. L.; Zeitler, U.; Maan, J. C.; Boebinger, G. S.; Kim, P.; Geim, A. K. *Science* **2007**, *315*, 1379–1379.

(10) Ozyilmaz, B.; Jarillo-Herrero, P.; Efetov, D.; Abanin, D. A.; Levitov, L. S.; Kim, P. *Phys. Rev. Lett.* **2007**, *99*, 166804.

(11) Bunch, J. S.; Yaish, Y.; Brink, M.; Bolotin, K.; McEuen, P. L. *Nano Lett.* **2005**, *5*, 287–290.

(12) Ryder, L. H. *Quantum Field Theory*; Cambridge University Press: Cambridge, U.K., 1985.

(13) Matulis, A.; Peeters, F. M. *Am. J. Phys.* **2009**, *77*, 595–601.

(14) Coulson, C. A. *Proc. Phys. Soc., London, Sect. A* **1953**, *66*, 652–655.

(15) Malysheva, L.; Onipko, A. *Phys. Rev. Lett.* **2008**, *100*, 186806.

(16) Onipko, A. *Phys. Rev. B: Condens. Matter Mater. Phys.* **2008**, *78*, 245412.

(17) Nikolaev, A. V.; Bibikov, A. V.; Avdeenkov, A. V.; Bodrenko, I. V.; Tkalya, E. V. *Phys. Rev. B: Condens. Matter Mater. Phys.* **2009**, *79*, 045418.

(18) Hod, O.; Peralta, J. E.; Scuseria, G. E. *Phys. Rev. B: Condens. Matter Mater. Phys.* **2007**, *76*, 233401.

(19) Ezawa, M. *Phys. Rev. B: Condens. Matter Mater. Phys.* **2007**, *76*, 245415.

(20) Hod, O.; Barone, V.; Peralta, J. E.; Scuseria, G. E. *Nano Lett.* **2007**, *7*, 2295–2299.

(21) Fernández-Rossier, J.; Palacios, J. J. *Phys. Rev. Lett.* **2007**, *99*, 177204.

(22) Shemella, P.; Zhang, Y.; Mailman, M.; Ajayan, P. M.; Nayak, S. K. *Appl. Phys. Lett.* **2007**, *91*, 042101.

(23) Ezawa, M. *Phys. E (Amsterdam, Neth.)* **2008**, *40*, 1421–1423. 17th International Conference on Electronic Properties of Two-Dimensional Systems.

(24) Hod, O.; Scuseria, G. E. *ACS Nano* **2008**, *2*, 2243–2249.

(25) Kudin, K. N. *ACS Nano* **2008**, *2*, 516–522.

(26) Hod, O.; Barone, V.; Scuseria, G. E. *Phys. Rev. B: Condens. Matter Mater. Phys.* **2008**, *77*, 035411.

(27) Jiang, D.; Chen, X.-Q.; Luo, W.; Shelton, W. A. *Chem. Phys. Lett.* **2009**, *483*, 120–123.

(28) Fujita, M.; Wakabayashi, K.; Nakada, K.; Kusakabe, K. *J. Phys. Soc. Jpn.* **1996**, *65*, 1920–1923.

(29) Wakabayashi, K.; Fujita, M.; Ajiki, H.; Sigrist, M. *Phys. Rev. B: Condens. Matter Mater. Phys.* **1999**, *59*, 8271–8282.

(30) Son, Y.-W.; Cohen, M. L.; Louie, S. G. *Phys. Rev. Lett.* **2006**, *97*, 216803.

(31) Zheng, H.; Wang, Z. F.; Luo, T.; Shi, Q. W.; Chen, J. *Phys. Rev. B: Condens. Matter Mater. Phys.* **2007**, *75*, 165414.

(32) Barone, V.; Hod, O.; Scuseria, G. E. *Nano Lett.* **2006**, *6*, 2748–2754.

(33) Son, Y.-W.; Cohen, M. L.; Louie, S. G. *Phys. Rev. Lett.* **2006**, *97*, 216803.

(34) Hsu, L.-Y.; Jin, B.-Y. *Chem. Phys.* **2009**, *355*, 177–182.

CT1000044